Latin American Journal of Solids and Structures
www.lajss.org

Parametric Modal Dynamic Analysis of Steel-Concrete Composite Beams with Deformable Shear Connection

Abstract

Composite structural elements of steel-concrete began to be used only in 1960 after the development of methods and constructive dispositions that ensured the functionality of these two materials together. In order to verify the importance of the participation of the axial mode in the frequency spectrum of the free vibration problem in composite beams with deformable shear connection, several analyses for 4 different boundary conditions and stiffness connection variation were performed.

The analysis of the problem was carried out by development and computational implementation of a finite element for composite beams with partial interaction in the longitudinal direction applied to the problem of free vibrations. The solutions to this problem in the literature are scarce, and project recommendations are simplified. The results show that the finite element exhibits an excellent performance compared with the analytical results and as the axial mode has a high modal contribution, despite the boundary condition and stiffness connection.

Keywords

Dynamic analysis, composite beams, deformable shear connection, Finite Elements Method, numerical analysis.

Wanderson G. Machado [a]
Francisco de A. Neves [b]
João Batista M. de Sousa Jr. [c]

a Universidade Federal Ouro Preto, Escola de Minas, Departamento de Engenharia Civil, Ouro Preto, MG, Brasil, wandersongonc@yahoo.com.br
b Universidade Federal Ouro Preto, Escola de Minas, Departamento de Engenharia Civil, Ouro Preto, MG, Brasil, fassis@em.ufop.br
c Universidade Federal do Ceará, Departamento de Engenharia Civil, Fortaleza, CE, Brasil, joaobatistasousajr@hotmail.com

http://dx.doi.org/10.1590/1679-78252981

Received 13.04.2016
In revised form 29.11.2016
Accepted 05.12.2016
Available online 09.12.2016

1 INTRODUCTION

Composite elements are becoming more popular in civil engineering structures, especially the composite elements of steel and concrete, formed by the association of profiles or steel plates with plates or linear elements of plain or reinforced concrete. The association seeks to obtain a structural element which combines the specific advantages of each material.

Steel and concrete are mechanically connected by the shear connectors. Thus, for the correct use of these structural elements it is necessary to understand the behavior of each element present in

the cross section as well as the behavior of all elements together, which is possible from the interaction provided by the longitudinal forces exerted by the connectors. There is a need for experimental and numerical assessments in order to provide a basis for better understanding of their behavior, and the objective of this work is to contribute in the field of numerical dynamic analysis of composite beams.

The most common steel-concrete composite structural elements are the composite column, the composite beam and the composite slab. Usually composite beams are idealized from an approximation of concrete slabs connected mechanically to steel beams by shear connectors (Figure 1), since composite beam solution is adopted in most of steel buildings. It takes advantage of the presence of the concrete slab cast over the steel beam, thereby forming a composite system with superior structural behavior when compared with the isolated steel beam. This improved structural behavior of the composite element, along with the growing use of steel structures in civil construction in Brazil has caused a significant increase in the use of this construction technique. This type of solution is also widely used when there are big spans as in bridges and industrial buildings. Some of the advantages of the composite beams compared with simple beams are: high ratio span versus beam height, less deformation and a high fundamental frequency of vibration (Nie et al., 2004).

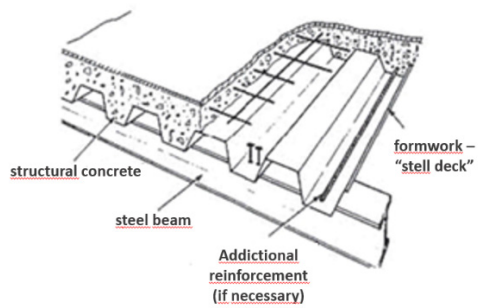

Figure 1: Composite floor shaped of composite slab associated with the steel beam.

The advantages of steel-concrete composite systems aside from those mentioned are: possibility of elimination of forms and shoring (depending on the adopted constructive sequence), reduced self-weight and volume of the structure, increased dimensional accuracy of the construction, reduced structural steel consumption, reduced protection against fire and corrosion, and increased stiffness and resistance to buckling (Queiroz et al., 2001). In composite beams one can also mention the prevention of buckling in the upper flange of the steel profile and buckling in the lateral side of the profile. Since they have their pre-manufactured steel elements, these systems have structural quality, accuracy and execution time lower than the structural systems in which all elements are molded in place.

The purpose of this article is to develop a numerical dynamic analysis of composite beams with partial interaction on the contact interface of the steel with the concrete, i.e. it allowing for a relative horizontal slip on the interface. The analysis consists in determining the natural frequencies and mode shapes from the variation of the connection stiffness, i.e., from the variation of interaction between steel and concrete, thus verifying the influence of interaction variation on the dynamic characteristics to be determined: natural frequencies and mode shapes.

The numerical simulation is made by the Finite Element Method (FEM), using an element with ten degrees of freedom, as used in the work of Dall'Asta and Zona (2004a), Silva (2006) and Oliveira (2009) for static analysis, which was adapted to solve dynamic analysis problems. The element used is based on Euler-Bernoulli's beam theory and considers the slip incorporated into its formulation.

The results for the Finite Element used in this article are compared to results obtained for elements developed by others and compared with analytical results (exact), in order to validate the efficiency of this element for the dynamic analysis of the composite beam problem.

In addition to the transverse mode shapes, this work aims to detect modes of axial vibration by checking their participation in the results obtained for the composite beam problem with partial interaction, as the connection stiffness is modified, i.e, longitudinal interaction is altered.

2 PARTIAL INTERACTION

Materials have natural adhesion, however, although it may be high, it is often not considered in the calculation of a structure due to its low reliability. For this reason, it becomes necessary to use elements, as shear connectors or other mechanical resources, in order to promote more interaction between interfaces of constituent materials of the composite element.

Shear connectors functions by absorbing the shearing efforts induced in the materials interface, providing a connection in the interface of both materials, decreasing longitudinal slip of the material (slip at the interface) and also vertical separation of the materials interface (displacement vertical).

The interaction in the interface can be partial or total. Under total interaction there is no slip in the interface or this slip is so small that can be neglected in the analysis, whereas in partial interaction, the slip has an important contribution to global behavior of the composite system or the structure in which the element is inserted, with effects on the analysis and design.

In this article, all analyses will be made considering the partial interaction at the materials interface of the steel-concrete composite beam. The partial interaction will be considered only in the horizontal direction, and total interaction is considered in the vertical direction, i.e., there is no vertical separation of the elements in the interface (uplift). Salari and Spacone (2001) reported that the reason of not considering the vertical separation is due to the absence of experimental evidence in composite beams analyses that prove its importance in the response.

There are several different devices that can be employed as shear connectors. A review of different types of connectors along with their main characteristics was presented by Shariati *et al.* (2012). Among these one can cite the headed stud bolt (Lee *et al.* 2005), the angle and channel connectors (Shariati *et al.*, 2013, Maleki and Bagheri, 2008, 2008a), the various types of perfobond connectors (Vellasco *et al.* 2007) and many recently proposed schemes (Shariati *et al.*,2012). The most frequently employed shear connectors in buildings are the headed stud bolts. In terms of dynamic analysis the connectors play an important role on the energy dissipation that takes place after dynamic excitations which may occur due to events such as seismic actions.

The scheme shown in Figure 2 refers to the displacements that occur in the composite beam, where u_1 and u_2 are the axial displacements, v_1 and v_2 are the vertical displacements, s is relative slip on the interface and ϑ is the rotation of the beam. As vertical separation shall not be considered, v_1 and v_2 are equal.

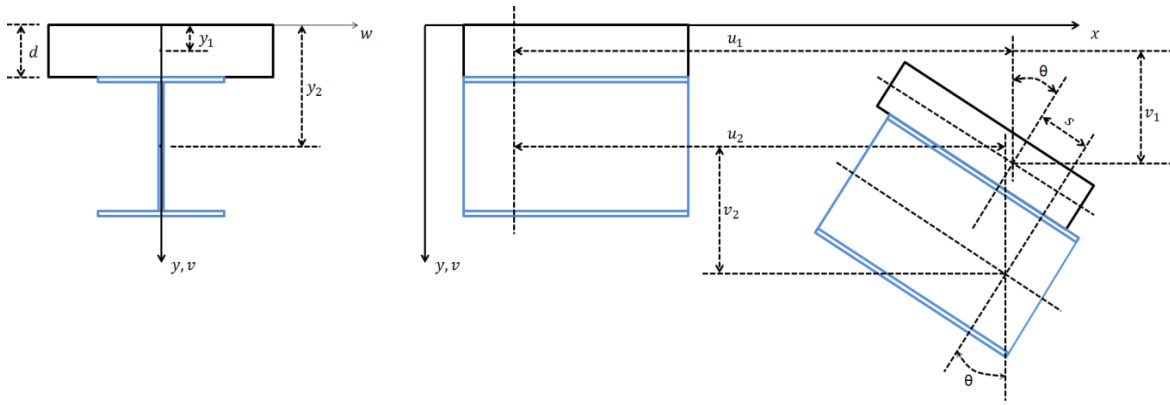

Figure 2: Displacements on the composite beam with incorporated slip.

According to Figure 2, the partial interaction on steel-concrete interface causes a slip in the interface given by:

$$s(x) = u_2 - u_1 + h\theta \tag{1}$$

where h is the distance between geometric centers of the cross sections corresponding to the constituent materials of the composite beam.

3 FREE VIBRATIONS PROBLEM

In the analysis of free vibration of a structure, there are two very important dynamic characteristics to be determined: natural frequencies and natural mode shapes.

Excluding damping, the equation of motion is given by:

$$\boldsymbol{M\ddot{d} + Kd = 0} \tag{2}$$

To find the natural frequencies and mode shapes, one should solve the classic eigenproblem:

$$(\boldsymbol{K} - {w_{n_j}}^2 \boldsymbol{M})\boldsymbol{\phi_j} = \boldsymbol{0} \tag{3}$$

where w_{nj} are the natural frequencies (eigenvalues) for each degree of freedom, obtained by the following polynomial equation:

$$\det \mid (\boldsymbol{K} - {w_{n_j}}^2 \boldsymbol{M}) \mid = \boldsymbol{0} \tag{4}$$

Mode shapes (eigenvectors) are obtained by substituting the values found in Equation 4 into Equation 3.

Normalization of eigenvectors leads to:

$$\overline{\boldsymbol{\phi}}_{\boldsymbol{j}} = \frac{\boldsymbol{\phi_j}}{\sqrt{{\boldsymbol{\phi_j}}^T \boldsymbol{M} \boldsymbol{\phi_j}}} \tag{5}$$

where ϕ_j is the eigenvector before normalization, and $\bar{\phi}_j$ is the normalized eigen vector.

The normalized modal matrix consisting of **N** mode shapes is given by:

$$\boldsymbol{\Phi} = \begin{bmatrix} \bar{\boldsymbol{\Phi}}_{1,1} & \cdot & \cdot & \cdot & \bar{\boldsymbol{\Phi}}_{1,N} \\ \cdot & \cdot & \cdot & \cdot & \cdot \\ \cdot & \cdot & \cdot & \cdot & \cdot \\ \cdot & \cdot & \cdot & \cdot & \cdot \\ \bar{\boldsymbol{\Phi}}_{N,1} & \cdot & \cdot & \cdot & \bar{\boldsymbol{\Phi}}_{N,N} \end{bmatrix} \tag{6}$$

4 FINITE ELEMENT FORMULATION FOR COMPOSITE BEAMS

Numerical solution via the finite element method for composite beam problems has raised he interest of many researchers around the world, and several works using elements of this type may be found, such as Oven et al. (1997), Faella et al. (2002), Salari and Spacone (2001) and Liang et al. (2004).

The solution for composite beam problem by using numerical methods becomes very interesting once these methods can be applied to all types of beams, including the more complex cases, for which there is no analytical solution. Numerical solution for the problem converges to analytic solution as the finite element mesh is refined.

4.1 Finite Element

The finite element used is composed of 10 degrees of freedom, with relative slide on the interface of its materials, named after Machado (2012) as "SLIP10DOF" as shown in Figure 3.

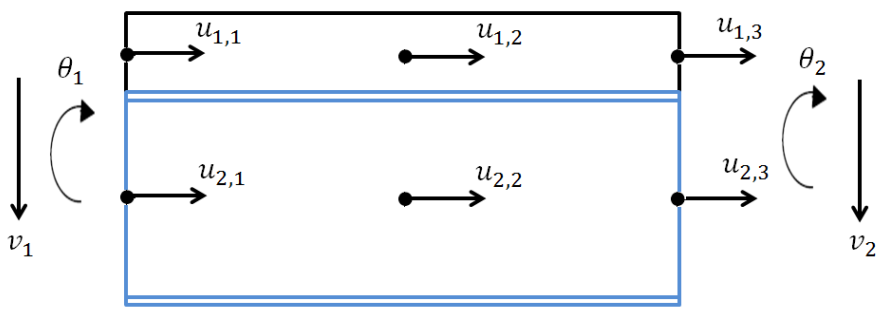

Figure 3: Degrees of freedom of the finite element "SLIP10DOF".

Where $u_{i,\,j}$, v_i e ϑ_i are axial displacements, vertical displacements and rotation, respectively, and the index i determines the type of material, where 1 corresponds to concrete and 2 corresponds to steel.

In order to model the problem of bar, a finite element bar model has the following kinematic assumptions associated with the deformation of an element of Euler-Bernoulli beam: interpolation

functions to ensure the continuity of the vertical and axial displacements, and rotations in the ends of the elements, where the latter are considered the same as those derived from the transverse displacements. To ensure these requirements, it must have at least a third degree polynomial for the transverse displacement, and at least linear for axial displacements. Presented below are the stiffness and mass matrices of the element.

4.2 Stiffness Matrix of the Element "SLIP10DOF"

First, the notation used for the deduction of the problem formulation is shown in Figure 4.

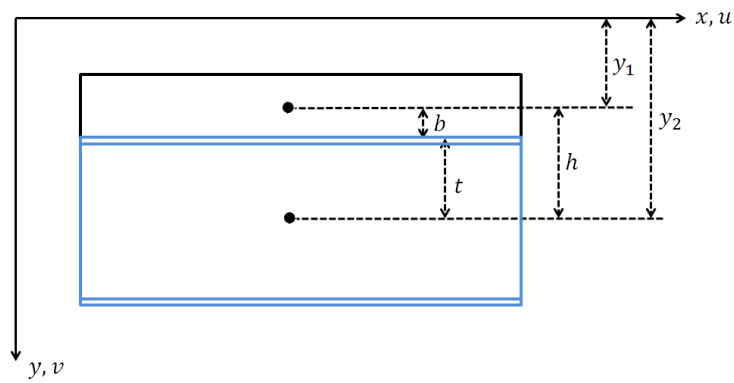

Figure 4: Distances to the axis of the element "SLIP10DOF".

The values y_1 and y_2 are respectively the distances from the x axis to the center of the concrete and steel sections, h is the distance between the centers of the sections, and b and t are respectively the distances of the centers of the concrete and steel sections to the contact interface of the materials and the super index *0* (zero) implies values at the reference axis.

Machado (2012) presents the expressions related to axial displacements u_1 and u_2, vertical displacement v e slip s identified in Figure 2.

According to kinematics, the expressions related to u_1, u_2, v and s are given respectively by:

$$u_1 = {u_1}^0 - (y - y_1)\theta = {u_1}^0(x) - (y - y_1)\theta(x) \tag{7}$$

$$u_2 = {u_2}^0 - (y - y_2)\theta = {u_2}^0(x) - (y - y_2)\theta(x) \tag{8}$$

$$v(x,y) = v^0(x) \tag{9}$$

$$s(x) = u_2(x, y_2 - t) - u_1(x, y_1 - b) = {u_2}^0(x) - {u_1}^0(x) + h\theta(x) \tag{10}$$

The total strain energy is given by the sum of the parts of axial strain of materials 1 and 2 to the portion of strain due to slip.

$$U = \int_V \frac{Ee^2}{2} dV + \int_V \frac{Fs^2}{2} dx \tag{11}$$

After calculating axial strain ε_1 and ε_2 for materials 1 and 2, concrete and steel, such as partial derivatives of the axial displacements u_1 and u_2, respectively, and replacing in Equation 11, the element strain energy in matrix form is obtained, incorporating the slip straining portions, given by:

$$U = \int_0^L \frac{1}{2} \left\langle {\varepsilon_1}^0 \quad {\varepsilon_2}^0 \quad k \quad s \right\rangle \begin{bmatrix} E_1A_1 & 0 & E_1S_1 & 0 \\ 0 & E_2A_2 & E_2S_2 & 0 \\ E_1S_1 & E_2S_2 & E_1I_1 + E_2I_2 & 0 \\ 0 & 0 & 0 & F \end{bmatrix} \begin{Bmatrix} {\varepsilon_1}^0 \\ {\varepsilon_2}^0 \\ k \\ s \end{Bmatrix} dx \tag{12}$$

where k is the connection stiffness.

In a more compact form, equation 12 can be given by:

$$U = \int_0^L \frac{1}{2} \boldsymbol{\varepsilon}(x)^T \boldsymbol{D} \boldsymbol{\varepsilon}(x) dx \tag{13}$$

where $\boldsymbol{\varepsilon}$ is the strain vector written as:

$$\boldsymbol{\varepsilon(x)} = \begin{Bmatrix} {\varepsilon_1}^0 \\ {\varepsilon_2}^0 \\ k \\ s \end{Bmatrix} = \begin{bmatrix} \frac{d}{dx} & 0 & 0 \\ 0 & \frac{d}{dx} & 0 \\ 0 & 0 & \frac{-d^2}{dx^2} \\ -1 & 1 & h\frac{d}{dx} \end{bmatrix} \begin{Bmatrix} {u_1}^0 \\ {u_2}^0 \\ v \end{Bmatrix} = \partial u(x) \tag{14}$$

and $\boldsymbol{D}$ is the matrix composed of physical and geometrical properties, where F is the force along the interaction.

The nodal displacements vector d of the finite element shown earlier in Figure 3 is:

$$\boldsymbol{d}^T = \left\langle {\boldsymbol{d}_{u_1}}^T \quad {\boldsymbol{d}_{u_2}}^T \quad {\boldsymbol{d}_v}^T \right\rangle \tag{15}$$

where $\boldsymbol{d}_{u_1}$ is the axial displacement vector of element 1, $\boldsymbol{d}_{u_2}$ is the axial displacement vector of element 2, and $\boldsymbol{d}_v$ the vertical displacement vector and rotations of elements 1 and 2, given by:

$${\boldsymbol{d}_{u_1}}^T = \left\langle u_{1,1} \quad u_{1,2} \quad u_{1,3} \right\rangle \tag{16}$$

$${\boldsymbol{d}_{u_2}}^T = \left\langle u_{2,1} \quad u_{2,2} \quad u_{2,3} \right\rangle \tag{17}$$

$${\boldsymbol{d}_v}^T = \left\langle v_1 \quad \theta_1 \quad v_2 \quad \theta_2 \right\rangle \tag{18}$$

where the superscript T involves the transposition of the vector or matrix.

One of the characteristics of formulation via MEF is the approach of the exact solution of displacements and stresses in the element by interpolation functions $\boldsymbol{N}$ of nodal displacements $\boldsymbol{d}$.

Discretizing by MEF, the axial and vertical displacements of the element, defined by the interpolation functions in the x coordinate, are respectively given by:

$$u_1 = \boldsymbol{N}_u(x)\boldsymbol{d}_{u_1} \tag{19}$$

$$u_2 = \boldsymbol{N}_u(x)\boldsymbol{d}_{u_2} \tag{20}$$

$$v = \boldsymbol{N}_v(x)\boldsymbol{d}_v \tag{21}$$

where $\boldsymbol{N}_u$ and $\boldsymbol{N}_v$ are interpolation functions in the x coordinate, and integration ends are 0 (zero) and L. These interpolation functions will be determined later for a general coordinate ξ.

In matrix form:

$$\boldsymbol{u}(x) = \boldsymbol{N}\boldsymbol{d} = \begin{bmatrix} \boldsymbol{N}_u(x) & \boldsymbol{0} & \boldsymbol{0} \\ \boldsymbol{0} & \boldsymbol{N}_u(x) & \boldsymbol{0} \\ \boldsymbol{0} & \boldsymbol{0} & \boldsymbol{N}_v(x) \end{bmatrix} \begin{Bmatrix} \boldsymbol{d}_{u_1} \\ \boldsymbol{d}_{u_2} \\ \boldsymbol{d}_v \end{Bmatrix} \tag{22}$$

After substituting the equation 22 in equation 14, the strain vector $\boldsymbol{\varepsilon}(x)$ is obtained as a function of the matrix which contains the derivatives of interpolation functions.

$$\varepsilon(x) = \boldsymbol{B}(x)\boldsymbol{d} \tag{23}$$

Substituting equation 23 into equation 12 or 13, in compact form, the strain energy is obtained, in terms of stiffness matrix,

$$U = \frac{1}{2}\boldsymbol{d}^T\boldsymbol{K}(x)\boldsymbol{d} \tag{24}$$

with the stiffness matrix given by:

$$\boldsymbol{K}(x) = \int_0^L \boldsymbol{B}(x)^T\boldsymbol{D}\boldsymbol{B}(x)dx \tag{25}$$

and $\boldsymbol{B}$ is a matrix obtained from the derivative of the interpolation matrix given by:

$$\boldsymbol{B}(x) = \begin{bmatrix} \boldsymbol{N}_{u,x} & \boldsymbol{0} & \boldsymbol{0} \\ \boldsymbol{0} & \boldsymbol{N}_{u,x} & \boldsymbol{0} \\ \boldsymbol{0} & \boldsymbol{0} & -\boldsymbol{N}_{u,xx} \\ \boldsymbol{N}_u & \boldsymbol{N}_u & h\boldsymbol{N}_{v,x} \end{bmatrix} \tag{26}$$

As functions are defined with respect to a generic element with general variable ξ along the axis, axial and transverse interpolation functions are given by:

$$\boldsymbol{N}_{u_1}{}^T = \boldsymbol{N}_{u_2}{}^T = \boldsymbol{N}_u{}^T = \begin{bmatrix} \frac{1}{2}\xi(\xi-1) \\ 1-\xi^2 \\ \frac{1}{2}\xi(\xi+1) \end{bmatrix} \tag{27}$$

$$\boldsymbol{N}_v{}^T = \begin{bmatrix} \frac{1}{2} - \frac{3}{4}\xi + \frac{1}{4}\xi^3 \\ \frac{L}{2}\left(\frac{1}{4} - \frac{1}{4}\xi - \frac{1}{4}\xi^2 + \frac{1}{4}\xi^3\right) \\ \frac{1}{2} + \frac{3}{4}\xi + \frac{1}{4}\xi^3 \\ \frac{L}{2}\left(-\frac{1}{4} - \frac{1}{4}\xi + \frac{1}{4}\xi^2 + \frac{1}{4}\xi^3\right) \end{bmatrix} \tag{28}$$

where the coordinates of their integration ends are -1 and 1, and

$$\xi = \frac{2}{L}x - 1 \tag{29}$$

Substituting the interpolation functions at the coordinate ξ (equations 27 and 28) in the matrix $\boldsymbol{B}(x)$, the matrix $\boldsymbol{B}(\xi)$ obtained is:

$$\boldsymbol{B}(x) = \begin{bmatrix} \boldsymbol{N}_{u,\xi}\frac{d\xi}{dx} & \boldsymbol{0} & \boldsymbol{0} \\ \boldsymbol{0} & \boldsymbol{N}_{u,\xi}\frac{d\xi}{dx} & \boldsymbol{0} \\ \boldsymbol{0} & \boldsymbol{0} & -\boldsymbol{N}_{v,\xi\xi}\left(\frac{d\xi}{dx}\right)^2 \\ \boldsymbol{N}_u & \boldsymbol{N}_u & h\boldsymbol{N}_{v,\xi}\frac{d\xi}{dx} \end{bmatrix} \tag{30}$$

where,

$$\frac{d\xi}{dx} = \frac{2}{L} \tag{31}$$

Therefore, the general Stiffness Matrix in function of ξ is given by:

$$\boldsymbol{K}(\xi) = \int_{-1}^{+1} \boldsymbol{B}(\xi)^T \boldsymbol{D}\boldsymbol{B}(\xi)\left(\frac{d\xi}{dx}\right)d\xi \tag{32}$$

4.3 Mass Matrix of the Element "SLIP10DOF"

Consistent Mass matrix for the described finite element is obtained from the expression of kinetic energy. After some algebraic manipulations, including the effects of rotational inertia matrix $\boldsymbol{M}$ is given by:

$$\boldsymbol{M} = \int_0^L \begin{bmatrix} \boldsymbol{m}_{u_1} & \boldsymbol{0} & \boldsymbol{m}_{u_1 v} \\ \boldsymbol{0} & \boldsymbol{m}_{u_2} & \boldsymbol{m}_{u_2 v} \\ -\boldsymbol{m}_{v u_1} & \boldsymbol{m}_{v u_2} & \boldsymbol{m}_{vv} \end{bmatrix} dx \tag{33}$$

where

$$\boldsymbol{m}_{u_1} = \int_0^L \rho_1 A_1 \boldsymbol{N}_u{}^T \boldsymbol{N}_u dx \tag{34}$$

$$\boldsymbol{m}_{u_2} = \int_0^L \rho_2 A_2 \boldsymbol{N}_u{}^T \boldsymbol{N}_u dx \tag{35}$$

$$\boldsymbol{m}_{u_1 v} = \int_0^L \rho_1 S_1 \boldsymbol{N}_u{}^T \boldsymbol{N}_{v,x} dx \tag{36}$$

$$\boldsymbol{m}_{u_2 v} = \int_0^L \rho_2 S_2 \boldsymbol{N}_u{}^T \boldsymbol{N}_{v,x} dx \tag{37}$$

$$\boldsymbol{m}_{v u_1} = \int_0^L \rho_1 S_2 \boldsymbol{N}_{v,x}{}^T \boldsymbol{N}_u dx \tag{38}$$

$$\boldsymbol{m}_{v u_2} = \int_0^L \rho_2 S_2 \boldsymbol{N}_{v,x}{}^T \boldsymbol{N}_u dx \tag{39}$$

$$\boldsymbol{m}_{vv} = \int_0^L \left(\rho_1 A_1 \boldsymbol{N}_v{}^T \boldsymbol{N}_v + \rho_1 I_1 \boldsymbol{N}_{v,x}{}^T \boldsymbol{N}_{v,x} \right) + \left(\rho_2 A_2 \boldsymbol{N}_v{}^T \boldsymbol{N}_v + \rho_2 I_2 \boldsymbol{N}_{v,x}{}^T \boldsymbol{N}_{v,x} \right) dx \tag{40}$$

where $\rho_1 I_1 \boldsymbol{N}_{v,x}{}^T \boldsymbol{N}_{v,x}$ is the inertia of the rotating section. If the axes are in the centroids, $\boldsymbol{m}_{u_1 v} = 0$ and $\boldsymbol{m}_{v u_1} = 0$, where ϱ, A, S and I are respectively the specific weight, area, static moment and inertia moment for materials 1 and 2.

Switching to the general coordinate "ξ", the mass matrix is given by:

$$\boldsymbol{M}(\xi) = \int_{-1}^{+1} \left[\boldsymbol{M}(\xi) \right] \frac{d\xi}{dx} d\xi \tag{41}$$

where,

$$\frac{dx}{d\xi} = \frac{1}{\frac{d\xi}{dx}} = \frac{L}{2} \tag{42}$$

5 NUMERICAL EXAMPLE

The example was based on Xu and Wu (2007) and is intended to determine two important parameters for composite beams dynamic analysis, natural frequencies and mode shapes with partial interaction, noting the influence of connection stiffness in these parameters.

The example to be solved is a composite beam, whose cross section is shown in Figure 5, and the which geometric and material properties of the cross section are as follows: L=4m, h=0.1m (distance between centers of gravity of the materials 1 and 2), E_1=12GPa, E_2=8GPa, A_1=0.015m², A_2=0.0075m², I_1=3.125x10-^{6}m^4, I_2=1.40625x10^{-4}m^4, m_1=36kg/m e m_2=3.75kg/m.

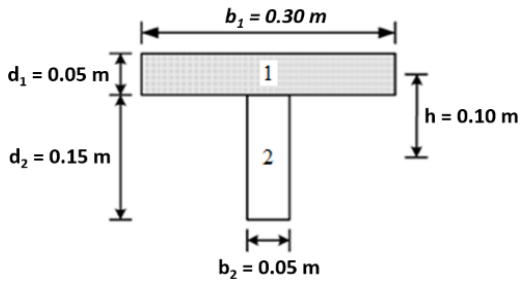

Figure 5: Composite beam.

Analysis of the parameters will be done for different connection stiffnesses, K_s, aiming to verify the influence of connection stiffness variation on the mode shape analysis. Therefore, for each analysis, the connection stiffness will assume the values of: 50MPa, 1 MPa, 0.1MPa and 0.01MPa.

Xu and Wu (2007) treated the same example for different boundary conditions. They have developed and solved analytically (exactly) the differential equations of the problem. Their analysis followed four scenarios: the first considered strain due to shear and rotation inertia. The second hypothesis considered only strain due to shear; the third considered only rotation inertia and, in the final analysis, neither of the two factors was considered.

Due to the assumptions made in the formulation of the finite element, strains due to shear are not considered in this work, but rotation inertia will be considered. So as in Xu and Wu (2007), analyses will be made to the four boundary conditions: simply supported, clamped - supported clamped - free and clamped - clamped.

5.1 Simply Supported Beam

Considering Ks = 50MPa, natural frequencies are determined and compared with the analytical results obtained by Xu and Wu (2007). Results will be obtained for a 15 mesh element since this quantity of finite elements has proved sufficient, and for fewer elements some values differed considerably from the exact values.

Considering the simply supported beam, the natural frequency obtained is given in Table 1:

Order	fn [Xu and Wu] (Hz)	fn [SLIP10DOF] (Hz)	Error (%)
1	10.3202	10.3035	0.1618
2	33.5087	33.4525	0.1677
3	66.4042	66.2852	0.1792
-	-	**92.2726**	-
4	109.9384	110.1022	0.1490
5	164.7303	164.8619	0.0799
6	231.0143	231.3543	0.1472
7	308.8379	309.6741	0.2708
-	-	**317.8041**	-
8	398.1566	400.0241	0.4690
9	498.8747	502.6015	0.7470
-	-	**563.1011**	-
-	-	**592.9015**	-
10	610.8634	617.7325	1.1245

Table 1: Natural frequencies for simply supported beam.

The obtained values indicate a good approximation to the values found by Xu and Wu (2007) showing that the finite element of ten degrees of freedom, SLIP10DOF, developed in Machado (2012), have good accuracy, since Xu and Wu (2007) values are exact (analytical), thus proving the efficiency of the element used.

In this work, as well as Machado (2012), frequencies corresponding to predominantly axial displacements were also determined, thereby resulting in axial shape modes of the beam. Axial frequency values are highlighted in Table 1, which are not determined by Xu and Wu (2007) in their analysis, since these authors considered only the transverse vibrations of the beam. On Table 1, one can see that for the simply supported beam, 4th natural frequency implies an axial mode shape, showing how important is the consideration of the axial mode.

In order to evaluate the influence of connection stiffness on dynamic characteristics (natural frequencies and mode shapes), a variation in the values of connection stiffness will be conducted, as shown in Table 2:

By reducing connection stiffness, or reducing the interaction at the interface, the axial mode shapes become more prevalent, coming to appear as the 1st mode shape when the connection stiffness value is in the order of 0.01Mpa. But a better analysis of the participation of these axial modes will be performed using the graphs contained in figures 6-9.

The axial mode found in this work led to evaluate participation (in percentage) of mode shapes in the results obtained, especially the participation of axial mode shape. For the numerical analysis, 15 SLIP10DOF elements were used, each element has 10 degrees of freedom in local system (Figure 3).

For each degree of freedom of the FE mesh one may associate not only a mode shape and its natural frequency but also a fraction of the system mass, hereby called effective mass. This value may be used as a measure of the participation of the respective vibration mode on the system response.

Order	fn [SLIP10DOF] for 50MPa (Hz)	fn [SLIP10DOF] for 1MPa (Hz)	fn [SLIP10DOF] for 0.1MPa (Hz)	fn [SLIP10DOF] for 0.01MPa (Hz)
1	10.3035	6.3367	6.0624	**2.7087**
2	33.4525	24.4315	**8.5309**	6.0333
3	66.2852	**25.9699**	24.1436	24.1143
4	**92.2726**	54.5420	54.2513	54.2221
5	110.1022	96.6460	96.3547	96.3254
6	164.8619	150.7205	150.4292	150.4000
7	231.3543	216.7654	**212.4280**	**211.4024**
8	309.6741	**222.5015**	216.4745	216.4454
9	**317.8041**	**286.8255**	**285.6492**	**285.5334**
10	400.0241	294.8245	294.5343	294.5053
11	502.6015	385.0064	384.7172	384.6883
12	**563.1011**	487.5040	487.2160	487.1872
13	**592.9015**	**571.6813**	**571.1165**	**571.0588**
14	617.7325	602.6086	602.3222	602.2935

Table 2: Natural frequencies for simply supported beam varying with the connection stiffness.

In order to better evaluate the influence of these axial modes in response for the problem, graphs below show the participation of each mode shape (in percentage). For this purpose, the effective mass of each mode shape were calculated and divided by the total mass of the system, finding the participation of each mode shape.

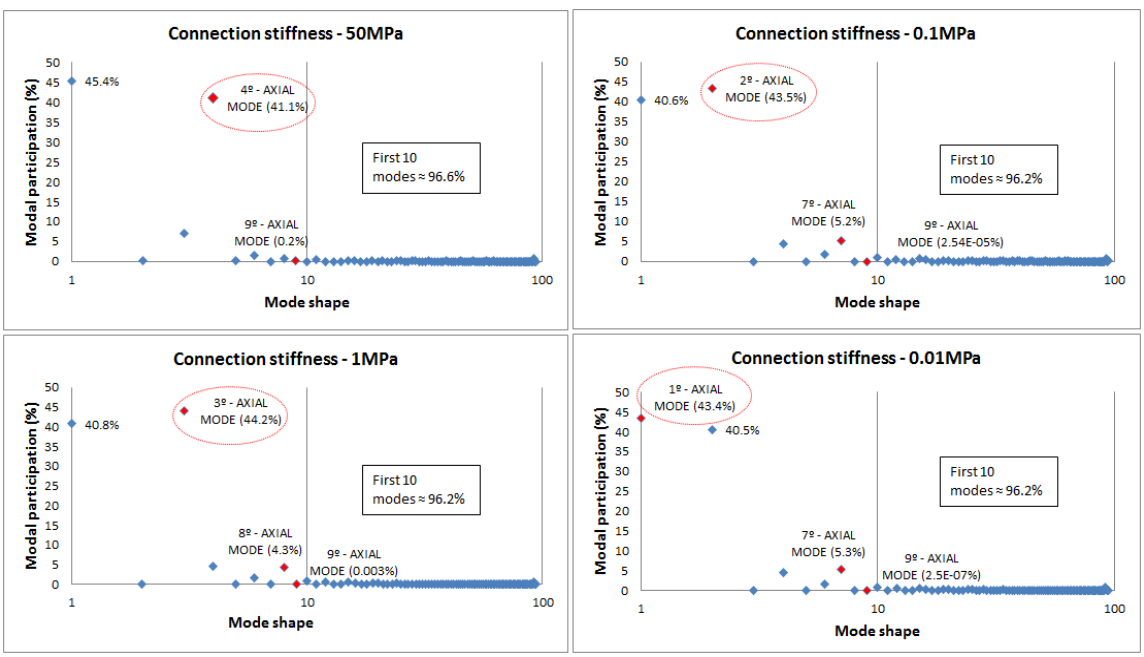

Figure 6: Mode shapes participation for different values of connection stiffness (beam simply supported).

Analyzing the graphs of Figure 6, one can see that the first mode shapes are responsible for almost all of the effective mass of the structure, so in an analysis to calculate the dynamic response via method of modal superposition, the contribution of these modes would be enough to obtaining accurate results. In order to illustrate, an analysis is made considering the first 10 modes, where they contribute in more than 96% of the system mass.

The participation values of AXIAL modes are highlighted, where it is clear that its modal participation is high even when the connection stiffness is high (41.1% for a stiffness of the 50MPa), and it is not necessary to decrease connection stiffness for it to play a crucial role. However, one notices that other axial modes appear as the connection stiffness is reduced, although with lower participation, but either way, showing the important role of these axial mode shapes.

5.2 Other Support Conditions

In order to verify the influence of support conditions with respect to modal participation and importance of axial mode when it varies the connection stiffness, several graphics for different stiffness are presented below.

5.2.1 Clamped-Free Beam

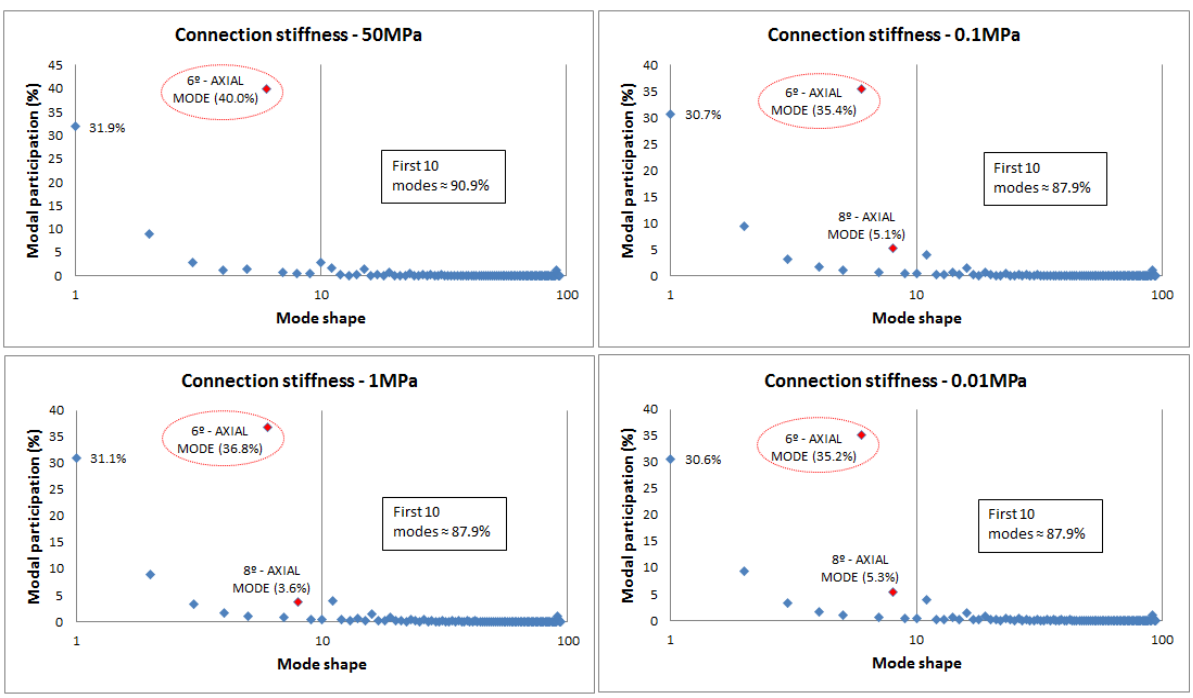

Figure 7: Mode shapes participation for different values of connection stiffness (clamped-free beam).

5.2.2 Clamped-Supported Beam

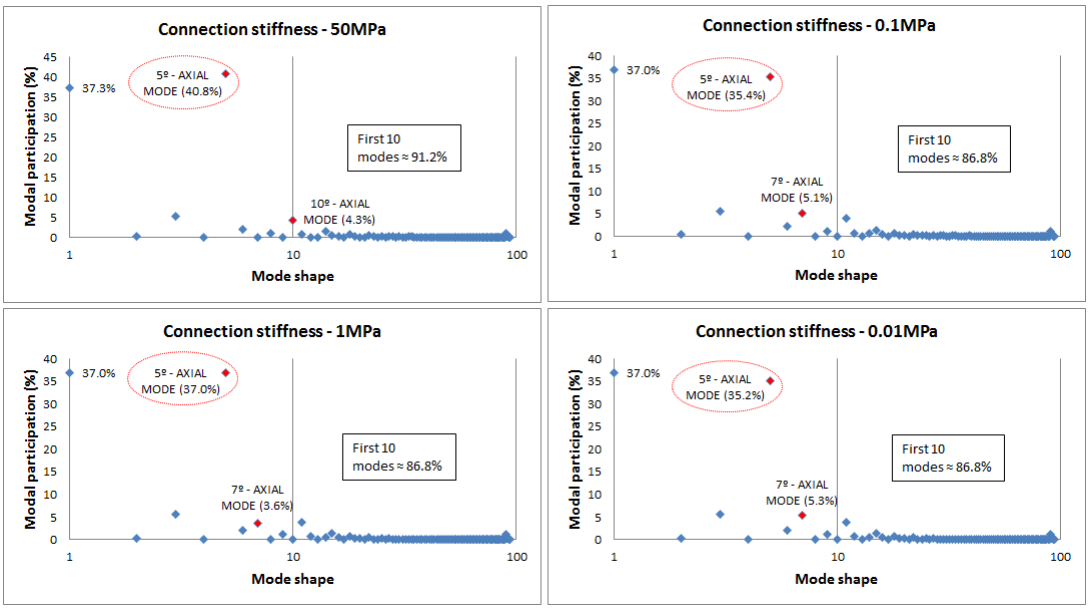

Figure 8: Mode shapes participation for different values of connection stiffness (clamped-supported beam).

5.2.3 Clamped-Clamped Beam

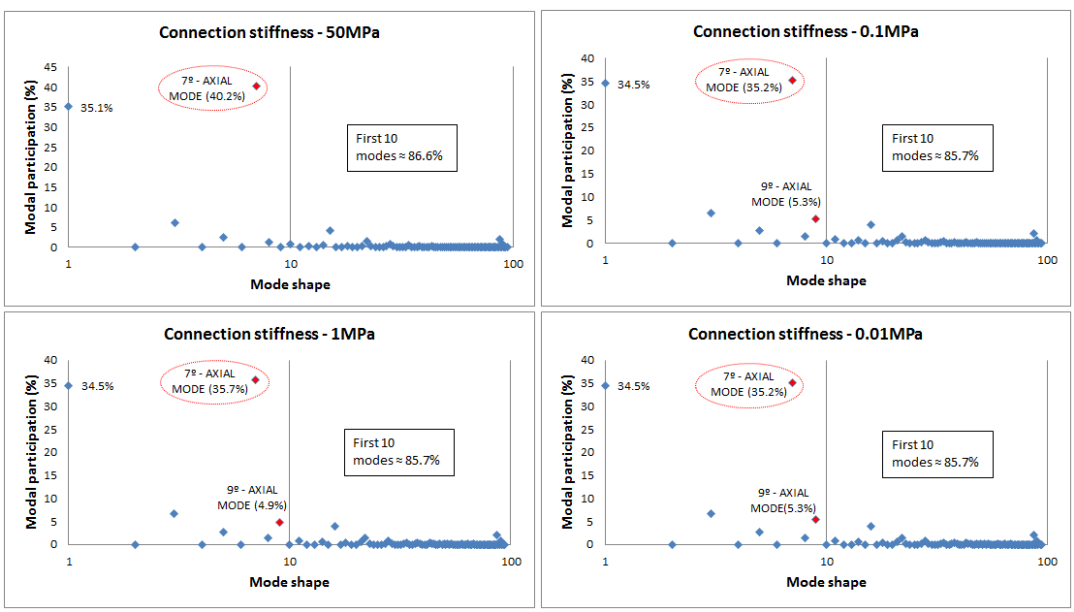

Figure 9: Mode shapes participation for different values of connection stiffness (clamped -clamped beam).

Similarly to what happens to the simply supported beam, for the other boundary conditions (Figures 7, 8 and 9), it is clear that there is a great influence of the axial mode shapes, and even as

it reduces the connection stiffness, more influences of axial modes arise. In fact, it is clear that there is a reduction in the order of appearance of axial mode when it reduces the connection stiffness of 50 to 1 MPa, and statistically no influence is perceived when it reduces to 0.01MPa.

5.3 Fundamental Frequency / Axial Frequency x Boundary Conditions x Connection Stiffness

Following, the influence of different boundary conditions on the fundamental frequency of vibration (Figure 10) will be evaluated, as well as the 1st axial frequency (Figure 11). The boundary conditions are analyzed: simply supported, clamped-free, clamped-supported and clamped-clamped, and the analysis made for a stiffness range of 0.001Mpa to 500Mpa.

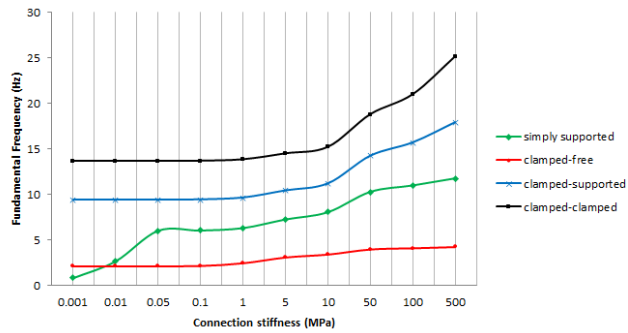

Figure 10: Assessment of the influence of different boundary conditions and stiffness on the Fundamental Frequency.

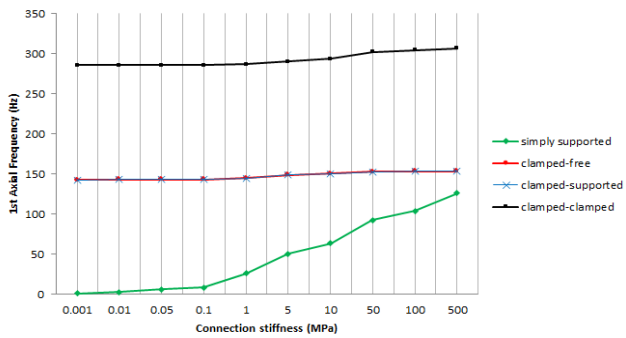

Figure 11: Assessment of the influence of different boundary conditions and stiffness on the 1st Axial Frequency.

From figure 10, it is clear that even a connection stiffness of about 10Mpa, the variation of fundamental frequency of vibration is very small for each boundary condition, except for the simply supported beam where it realizes considerable variation for the first stiffness analyzed (0.001 to 0.05Mpa) and then maintains the same behavior as other boundary conditions to the stiffness of 10Mpa. Above the stiffness of 10 MPa, it is clear that for the clamped-free conditions practically continues with no change in its fundamental vibration frequency even with a large increase in stiffness, as for the other boundary conditions there is considerable variation, especially in clamped-clamped, where the frequency variation was greater in the stiffness range analyzed.

About Figure 11, it can be said that the variation of the 1st frequency of axial vibration in relation to boundary conditions and variation of stiffness is too small for the clamped-supported beam, clamped-free and clamped-clamped beam. However, for the simply supported condition, it is clear that from the 0.1MPa stiffness, there is a wide variation with the stiffness variation, showing that the axial frequency has greater influence for simply supported beams, as it is easily perceived in the analysis of figures 6-9, where it was shown the appearance of axial modes for different boundary conditions and it was verified that for the simply supported condition, 1st axial mode emerged as a fundamental frequency for the stiffness of 0.01Mpa (Figure 6). It is also observed that for clamped-free and clamped-supported conditions, the values of the first axial frequencies for the different stiffness are practically equal.

6 CONCLUSIONS

SLIP10DOF element developed and implemented by Machado (2012) to composite beams, considering the partial interaction applied to the problem of free vibrations, showed an excellent performance when compared with the analytical results and other numerical approaches available in the literature.

With the variation of the connection stiffness and boundary conditions (support), it can be seen clearly how these boundary conditions influence the axial vibration modes. One sees clearly the importance of considering the axial mode, since for all analyses with different boundary conditions and variation in connection stiffness, modal contribution of this mode varies approximately 35-44%, particularly for simply supported beams, where there is a contribution of around 44% regardless of the connection stiffness value. Also for the simply supported case, one can note that as the connection stiffness reduces, the order corresponding to the appearance of axial mode decreases, so that for stiffness equals to 0.01MPa, axial mode frequency appears as fundamental vibration. This was not observed for the other boundary conditions.

Another point worth mentioning is the emergence of other axial modes, of a higher order, when connection stiffness reduces. It appears that first 10 mode shapes are responsible for modal contribution of 86-97% when considering all boundary conditions versus the variation of the connection stiffness. Moreover, the axial modes for all variations of boundary conditions and connection stiffness contributed 40-48% in the modal participation.

It can be conclude therefore that the axial modes are important contributions to the vibration system and must be considered in the calculation of response to a dynamic analysis to obtain good results.

The variation of the first axial mode frequency is negligible for boundary conditions other than the simply-supported case, for which already for very low values of the shear connection (0,01 MPa) displays an important variation with the connection stiffness.

According to EUROCODE 4, “Ductile connectors are those with sufficient deformation capacity to justify the assumption of ideal plastic behavior of the shear connection in the structure considered”. Although this work does not take into consideration the ductility of the connectors, it is expected in general an increase of the structural damping rate (hysteretic damping) when cyclic dynamic load is applied for this type of structural system with ductile connectors. Especially when you

have a low degree of partial shear connection (low degree of interaction). This is in accordance with the researches conducted by Bursi and Gramola (2000) and Bursi et al. (2005).

Acknowledgments

The authors thank CNPq, CAPES, FAPEMIG and UFOP, for their support for this work.

References

Bursi, O.S., Gramola, G. (2000). Behaviour of composite substructures with full and partial shear connection under quasi-static cyclic and pseudo-dynamic displacements. Materials and Structures/Materiaux et Constructions, 33 (3), 154-163, dx.doi.org/10.1007/BF02479409.

Bursi, O.S., Sunb, F.-F., Postal, S. (2005). Non-linear analysis of steel–concrete composite frames with full and partial shear connection subjected to seismic loads. Journal of Constructional Steel Research, 61 (1), 67–92, dx.doi.org/10.1016/j.jcsr.2004.06.002.

Dall'Asta, A., Zona, A. (2004a). Slip Locking in Finite Elements for Composite Beams with Deformable Shear Connection. Finite Elements in Analysis and Design, 40 (13-14), 1907-1930, dx.doi.org/10.1016/j.finel.2004.01.007.

Eurocode 4 (2004). Design of composite structures (ENV 1994)' Part 1-1/1992 General rules and rules for buildings", CEN Publications, Brussels, Belgium.

Faella, C., Martinelli, E., Nigro, E. (2002). Steel and Concrete Composite Beam with Flexible Shear Connection: "Exact" Analytical Expression of the Stiffness Matrix and Applications. Computer & Structures, 80 (11),1001-09, dx.doi.org/10.1016/S0045-7949(02)00038-X

Lee, P., Shim, C., Chang, S. (2005). Static and fatigue behavior of large stud shear connectors for steel-concrete composite bridges. Journal of Constructional Steel Research, 61(9), 1270-1285, dx.doi.org/10.1016/j.jcsr.2005.01.007.

Liang, Q.Q., Uy, B., Bradford, M.A., Ronagh, H.R. (2004). Ultimate Strength of Continuous Composite Beams in Combined Bending and Shear. Journal of Constructional Steel Research, 60(8), 1109-28, dx.doi.org/10.1016/j.jcsr.2003.12.001.

Machado, W.G. (2012). Análise Dinâmica de Vigas Mistas com Interação Parcial (Dynamic Analysis of Composite Beams with Partial Interaction), MSc Dissertation, Department of Civil Engineering, Escola de Minas, Federal University of Ouro Preto (in Portuguese). Available at www.propec.ufop.br.

Maleki, S., Bagheri, S. (2008) Behavior of channel shear connectors, Part I: Experimental study, Journal of Constructional Steel Research, 64(12), 1333-1340, dx.doi.org/10.1016/j.jcsr.2008.01.010.

Maleki, S., Bagheri, S. (2008a). Behavior of channel shear connectors, Part II: Analytical study Journal of Constructional Steel Research, 64(12), 1341-1348, dx.doi.org/10.1016/j.jcsr.2008.01.006.

Maleki, S., Mahoutian, M. (2009) Experimental and analytical study on channel shear connectors in fiber-reinforced concrete, Journal of Constructional Steel Research, 65 (8-9), 1787-1793, dx.doi.org/10.1016/j.jcsr.2009.04.008.

Nie, J.F., Cai, C.S. (2004). Stiffiness and Deflection of Steel-Concrete Composite Beams under Negative Bending. Journal of Structural Engineering, 130 (11), 1842 -51, dx.doi.org/10.1061/(ASCE)0733-944.

Oehlers, D.J., Bradford, M.A. (1999). Elementary Behaviour of Composite Steel ans Concrete Structural Members. Oxford: Butterworth Heinemann.

Oliveira, C.E. (2009). Análise Não-Linear Geométrica de Vigas-Colunas com Interação Parcial (Nonlinear Analysis of Geometric Beam-columns with Partial Interaction), MSc Dissertation, Department of Civil Engineering, Escola de Minas, Federal University of Ouro Preto (in Portuguese). Available at www.propec.ufop.br.

Oven, V.A., Burgess, I.W., Plan, K.R.J., Wali, A.A. (1997). An analytical Model for the Analysis of Composite Beam with Parcial Interaction. Computer & Structures, 62 (3),493 -504, dx.doi.org/10.1016/S0045-7949(97)80001-2.

Queiroz, G., Pimenta, R.J., Da Mata, L.A. (2001). Elementos das Estruturas Mistas Aço-Concreto (Elements of Composite Structures Steel-Concrete). Belo Horizonte: O Lutador (in Portuguese).

Salari, M.R., Spacone, E. (2001). Finite Element Formulations of One-Dimensional Elements with Bond-slip. Eng. Struct., 23 (7), 815–26, dx.doi.org/10.1016/S0141-0296(00)00094-8.

Shariati, A., Sulong, N.H.R., Suhatril, M., Shariati, M. (2012). Various types of shear connectors in composite structures: A review. International Journal of Physical Sciences ,7(22), 2876-2890, dx.doi.org/10.13140/RG.2.1.1903.0563

Shariati, M., Sulong, N.H.R., Suhatril, M., Shariati, A., Arabnejad Khanouki, M.M., Sinaei, H. (2013) Comparison of behaviour between channel and angle shear connectors under monotonic and fully reversed cyclic loading, Construction and Building Materials, 38, 582-593, dx.doi.org/10.1016/j.conbuildmat.2012.07.050.

Vellasco, P., De Andrade, S., Ferreira, L., De Lima, L. (2007). Semi-rigid composite frames with perfobond and T-rib connectors Part 1: Full scale tests. Journal of Constructional Steel Research, 63 (2), 263-279, dx.doi.org/10.1016/j.jcsr.2006.04.011

Xu, R., Wu, Y. (2007). Static, dynamic and buckling analysis of partial interaction composite members using Timoshenko's beam theory. International Journal of Mechanical Sciences, 49 (10), 1139–55, dx.doi.org/10.1016/j.ijmecsci.2007.02.006.

APPENDIX

Analytical Arrays (Element "SLIP 10DOF")

As the design for the stiffness, mass and damping matrices for "SLIP10DOF" element was introduced, the analytical matrices are presented below.

Stiffness matrix is composed of two parts (due to the strain and due to the slip), as described in Equation 11.

According to Machado (2012), the portion of the stiffness matrix due to strain (ε_1 and ε_2), are given respectively by:

$$\boldsymbol{K}_{\varepsilon,1} = \begin{bmatrix} \frac{7E_1A_1}{3L} & \frac{-8E_1A_1}{3L} & \frac{E_1A_1}{3L} & 0 & 0 & 0 & 0 & 0 & 0 & 0 \\ \frac{-8E_1A_1}{3L} & \frac{16E_1A_1}{3L} & \frac{-8E_1A_1}{3L} & 0 & 0 & 0 & 0 & 0 & 0 & 0 \\ \frac{E_1A_1}{3L} & \frac{-8E_1A_1}{3L} & \frac{7E_1A_1}{3L} & 0 & 0 & 0 & 0 & 0 & 0 & 0 \\ 0 & 0 & 0 & 0 & 0 & 0 & 0 & 0 & 0 & 0 \\ 0 & 0 & 0 & 0 & 0 & 0 & 0 & 0 & 0 & 0 \\ 0 & 0 & 0 & 0 & 0 & 0 & 0 & 0 & 0 & 0 \\ 0 & 0 & 0 & 0 & 0 & 0 & \frac{12E_1I_1}{L^3} & \frac{6E_1I_1}{L^2} & \frac{-12E_1I_1}{L^3} & \frac{6E_1I_1}{L^2} \\ 0 & 0 & 0 & 0 & 0 & 0 & \frac{6E_1I_1}{L^2} & \frac{4E_1I_1}{L} & \frac{-6E_1I_1}{L^2} & \frac{2E_1I_1}{L} \\ 0 & 0 & 0 & 0 & 0 & 0 & \frac{-12E_1I_1}{L^3} & \frac{-6E_1I_1}{L^2} & \frac{12E_1I_1}{L^3} & \frac{-6E_1I_1}{L^2} \\ 0 & 0 & 0 & 0 & 0 & 0 & \frac{6E_1I_1}{L^2} & \frac{2E_1I_1}{L} & \frac{-6E_1I_1}{L^2} & \frac{4E_1I_1}{L} \end{bmatrix} \quad (43)$$

$$\boldsymbol{K}_{\varepsilon,1} = \begin{bmatrix} 0 & 0 & 0 & 0 & 0 & 0 & 0 & 0 & 0 & 0 \\ 0 & 0 & 0 & 0 & 0 & 0 & 0 & 0 & 0 & 0 \\ 0 & 0 & 0 & 0 & 0 & 0 & 0 & 0 & 0 & 0 \\ 0 & 0 & 0 & \frac{7E_1A_1}{3L} & \frac{-8E_1A_1}{3L} & \frac{E_1A_1}{3L} & 0 & 0 & 0 & 0 \\ 0 & 0 & 0 & \frac{-8E_1A_1}{3L} & \frac{16E_1A_1}{3L} & \frac{-8E_1A_1}{3L} & 0 & 0 & 0 & 0 \\ 0 & 0 & 0 & \frac{E_1A_1}{3L} & \frac{-8E_1A_1}{3L} & \frac{7E_1A_1}{3L} & 0 & 0 & 0 & 0 \\ 0 & 0 & 0 & 0 & 0 & 0 & \frac{12E_1I_1}{L^3} & \frac{6E_1I_1}{L^2} & \frac{-12E_1I_1}{L^3} & \frac{6E_1I_1}{L^2} \\ 0 & 0 & 0 & 0 & 0 & 0 & \frac{6E_1I_1}{L^2} & \frac{4E_1I_1}{L} & \frac{-6E_1I_1}{L^2} & \frac{2E_1I_1}{L} \\ 0 & 0 & 0 & 0 & 0 & 0 & \frac{-12E_1I_1}{L^3} & \frac{-6E_1I_1}{L^2} & \frac{12E_1I_1}{L^3} & \frac{-6E_1I_1}{L^2} \\ 0 & 0 & 0 & 0 & 0 & 0 & \frac{6E_1I_1}{L^2} & \frac{2E_1I_1}{L} & \frac{-6E_1I_1}{L^2} & \frac{4E_1I_1}{L} \end{bmatrix} \tag{44}$$

where the stiffness matrix total due to deformation, $\boldsymbol{K}_{\varepsilon}$, is given by the sum of Equations 43 and 44.

The portion of the stiffness matrix due to slip, $\boldsymbol{K}_s$ (Machado, 2012) is given by:

$$K_s = \begin{bmatrix} K_{s,1} & -K_{s,1} & K_{s,2} \\ -K_{s,1} & K_{s,1} & -K_{s,2} \\ \left(K_{s,2}\right)^T & \left(-K_{s,2}\right)^T & \left(K_{s,3}\right)^T \end{bmatrix} \tag{45}$$

where $\boldsymbol{K}_{s,1}$, $\boldsymbol{K}_{s,2}$ and $\boldsymbol{K}_{s,3}$ were determined only to simplify Equation 45, therefore:

$$\boldsymbol{K}_{s,1} = \begin{bmatrix} \frac{2FL}{15} & \frac{FL}{15} & \frac{-FL}{30} \\ \frac{FL}{15} & \frac{8FL}{15} & \frac{FL}{15} \\ \frac{-FL}{30} & \frac{FL}{15} & \frac{2FL}{15} \end{bmatrix} \tag{46}$$

$$\boldsymbol{K}_{s,2} = \begin{bmatrix} \frac{Fh}{10} & \frac{-7FhL}{60} & -\frac{Fh}{10} & \frac{FhL}{20} \\ \frac{4Fh}{5} & \frac{FhL}{15} & -\frac{4Fh}{5} & \frac{FhL}{15} \\ \frac{Fh}{10} & \frac{FhL}{20} & -\frac{Fh}{10} & \frac{-7FhL}{60} \end{bmatrix} \tag{47}$$

$$\boldsymbol{K}_{s,3} = \begin{bmatrix} \frac{6Fh^2}{5L} & \frac{Fh^2}{10} & -\frac{6Fh^2}{5L} & \frac{Fh^2}{10} \\ \frac{Fh^2}{10} & \frac{2Fh^2L}{15} & -\frac{Fh^2}{10} & -\frac{Fh^2L}{30} \\ -\frac{6Fh^2}{5L} & -\frac{Fh^2}{10} & \frac{6Fh^2}{5L} & -\frac{Fh^2}{10} \\ \frac{Fh^2}{10} & -\frac{Fh^2L}{30} & -\frac{Fh^2}{10} & \frac{2Fh^2L}{15} \end{bmatrix} \tag{48}$$

Thus the stiffness matrix element ($\boldsymbol{K}$) is given by the sum of the parts, that is, the sum of Equations 43-45. The mass matrix($\boldsymbol{M}$) is given by Equation 41, where their mass portions are given by:

$$\boldsymbol{m}_{u1} = \begin{bmatrix} \frac{2\rho_1 A_1 L}{15} & \frac{\rho_1 A_1 L}{15} & \frac{-\rho_1 A_1 L}{30} \\ \frac{\rho_1 A_1 L}{15} & \frac{8\rho_1 A_1 L}{15} & \frac{\rho_1 A_1 L}{15} \\ \frac{-\rho_1 A_1 L}{30} & \frac{\rho_1 A_1 L}{15} & \frac{2\rho_1 A_1 L}{15} \end{bmatrix} \tag{49}$$

$$\boldsymbol{m}_{u2} = \begin{bmatrix} \frac{2\rho_2 A_2 L}{15} & \frac{\rho_2 A_2 L}{15} & \frac{-\rho_2 A_2 L}{30} \\ \frac{\rho_2 A_2 L}{15} & \frac{8\rho_2 A_2 L}{15} & \frac{\rho_2 A_2 L}{15} \\ \frac{-\rho_2 A_2 L}{30} & \frac{\rho_2 A_2 L}{15} & \frac{2\rho_2 A_2 L}{15} \end{bmatrix} \tag{50}$$

$$\boldsymbol{m}_{u_1 v} = \begin{bmatrix} -\frac{\rho_1 S_1}{10} & \frac{7\rho_1 S_1 L}{60} & \frac{\rho_1 S_1}{10} & -\frac{\rho_1 S_1 L}{20} \\ -\frac{4\rho_1 S_1}{5} & -\frac{\rho_1 S_1 L}{15} & \frac{4\rho_1 S_1}{5} & -\frac{\rho_1 S_1 L}{15} \\ -\frac{\rho_1 S_1}{10} & -\frac{\rho_1 S_1 L}{20} & \frac{\rho_1 S_1}{10} & \frac{7\rho_1 S_1 L}{60} \end{bmatrix} \tag{51}$$

$$\boldsymbol{m}_{u_2 v} = \begin{bmatrix} -\frac{\rho_2 S_2}{10} & \frac{7\rho_2 S_2 L}{60} & \frac{\rho_2 S_2}{10} & -\frac{\rho_2 S_2 L}{20} \\ -\frac{4\rho_2 S_2}{5} & -\frac{\rho_2 S_2 L}{15} & \frac{4\rho_2 S_2}{5} & -\frac{\rho_2 S_2 L}{15} \\ -\frac{\rho_2 S_2}{10} & -\frac{\rho_2 S_2 L}{20} & \frac{\rho_2 S_2}{10} & \frac{7\rho_2 S_2 L}{60} \end{bmatrix} \tag{52}$$

$$\boldsymbol{m}_{v u_1} = \left(\boldsymbol{m}_{u_1 v}\right)^T \tag{53}$$

$$\boldsymbol{m}_{v u_2} = \left(\boldsymbol{m}_{u_2 v}\right)^T \tag{54}$$

$$\boldsymbol{m}_{vv} = \boldsymbol{m}_{vv1} + \boldsymbol{m}_{vv2}\,\mathrm{x} \tag{55}$$

where,

$$\boldsymbol{m}_{vv1} = \begin{bmatrix} \frac{13\rho_1 A_1 L}{35} + \frac{6\rho_1 I_1}{5L} & \frac{11\rho_1 A_1 L^2}{210} + \frac{\rho_1 I_1}{10} & \frac{9\rho_1 A_1 L}{70} - \frac{6\rho_1 I_1}{5L} & -\frac{13\rho_1 A_1 L^2}{420} + \frac{\rho_1 I_1}{10} \\ \frac{11\rho_1 A_1 L^2}{210} + \frac{\rho_1 I_1}{10} & \frac{\rho_1 A_1 L^2}{105} + \frac{2\rho_1 I_1 L}{15} & \frac{13\rho_1 A_1 L^2}{420} - \frac{\rho_1 I_1}{10} & -\frac{\rho_1 A_1 L^2}{140} - \frac{\rho_1 I_1 L}{30} \\ \frac{9\rho_1 A_1 L}{70} - \frac{6\rho_1 I_1}{5L} & \frac{13\rho_1 A_1 L^2}{420} - \frac{\rho_1 I_1}{10} & \frac{13\rho_1 A_1 L}{35} + \frac{6\rho_1 I_1}{5L} & -\frac{11\rho_1 A_1 L^2}{210} - \frac{\rho_1 I_1}{10} \\ -\frac{13\rho_1 A_1 L^2}{420} + \frac{\rho_1 I_1}{10} & -\frac{\rho_1 A_1 L^2}{140} - \frac{\rho_1 I_1 L}{30} & -\frac{11\rho_1 A_1 L^2}{210} - \frac{\rho_1 I_1}{10} & \frac{\rho_1 A_1 L^2}{105} + \frac{2\rho_1 I_1 L}{15} \end{bmatrix} \tag{56}$$

$$\boldsymbol{m}_{vv1} = \begin{bmatrix} \frac{13\rho_2 A_2 L}{35} + \frac{6\rho_2 I_2}{5L} & \frac{11\rho_2 A_2 L^2}{210} + \frac{\rho_2 I_2}{10} & \frac{9\rho_2 A_2 L}{70} - \frac{6\rho_2 I_2}{5L} & -\frac{13\rho_2 A_2 L^2}{420} + \frac{\rho_2 I_2}{10} \\ \frac{11\rho_2 A_2 L^2}{210} + \frac{\rho_2 I_2}{10} & \frac{\rho_2 A_2 L^2}{105} + \frac{2\rho_2 I_2 L}{15} & \frac{13\rho_2 A_2 L^2}{420} - \frac{\rho_2 I_2}{10} & -\frac{\rho_2 A_2 L^2}{140} - \frac{\rho_2 I_2 L}{30} \\ \frac{9\rho_2 A_2 L}{70} - \frac{6\rho_2 I_2}{5L} & \frac{13\rho_2 A_2 L^2}{420} - \frac{\rho_2 I_2}{10} & \frac{13\rho_2 A_2 L}{35} + \frac{6\rho_2 I_2}{5L} & -\frac{11\rho_2 A_2 L^2}{210} - \frac{\rho_2 I_2}{10} \\ -\frac{13\rho_2 A_2 L^2}{420} + \frac{\rho_2 I_2}{10} & -\frac{\rho_2 A_2 L^2}{140} - \frac{\rho_2 I_2 L}{30} & -\frac{11\rho_2 A_2 L^2}{210} - \frac{\rho_2 I_2}{10} & \frac{\rho_2 A_2 L^2}{105} + \frac{2\rho_2 I_2 L}{15} \end{bmatrix} \tag{57}$$

Substituting the Equations 49-57 into Equation 41, there is the matrix mass (***M***) of "SLIP10DOF" element.